Jovana Mandić[1,a], Maja Mladenović[1], Dragana Lazić[1], Igor Radisavljević[1], Dragomir Glišić[2], Nada Ilić[1]

INFLUENCE OF CHANGES IN THE MICROSTRUCTURE OF THE WELDED JOINT DUE TO FRICTION STIR WELDING OF ALUMINIUM ALLOYS 2024 AND 5083 ON THE ELECTRICAL CONDUCTIVITY AND ELECTROCHEMICAL PARAMETERS IN CORROSIVE ENVIRONMENTS

UTICAJ PROMENE MIKROSTRUKTURE ZAVARENOG SPOJA USLED ZAVARIVANJA TRENJEM ALATOM LEGURA ALUMINIJUMA 2024 I 5083 NA ELEKTRIČNU PROVODLJIVOST I ELEKTROHEMIJSKE PARAMETRE U KOROZIONIM SREDINAMA

Original scientific paper / Originalni naučni rad

Paper received / Rad primljen:

August 2022.

Paper accepted / Rad prihvaćen:

January 2023

Author's address / Adresa autora:

[1]Military Technical Institute, Ratka Resanovića 1, 11000 Beograd, Republic of Serbia

[2]University of Belgrade, Faculty of Technology and Metallurgy, Karnegijeva 4, 11120 Beograd, Republic of Serbia

email: *[a] jmandic96@gmail.com*

Keywords: friction stir welding, weld characterization, alloy 2024-T351, alloy 5083-H111

Ključne reči: zavarivanje trenjem alatom, karakterizacija zavarenog spoja, legura 2024-T351,legura 5083-H111

Abstract

In this paper physical and metallographic properties of a dissimilar aluminium alloy friction-stir-welded joint (FSW) of non-heat treated aluminium alloy 5083-H111 as well as heat treated aluminium alloy 2024-T351 are examined. The chosen tool for welding had a standard screw thread radius, and for the welding parameters the ratio R/v = 750/73 was chosen. In order to determine the change in electrical conductivity and electrochemical parameters of the base materials and the welded joint in corrosive environments depending on the change in microstructure due to welding, metallographic analysis of the welded joint on an optical microscope was performed, and electrical conductivity and electrochemical parameters of the base material and the welded joint were also examined.

Rezime

U ovom radu ispitane su fizičke i metalografske osobine raznorodnog zavarenog spoja legure aluminijuma 5083-H111, koja se termički ne obrađuje, i legure aluminijuma 2024-T351, koja se termički obrađuje, dobijenog postupkom zavarivanja trenjem alatom (Friction Stir Welding-FSW). Zavarivanje je izvršeno pomoću alata standardnog radijusa navoja, sa parametrima Vrot/Vzav = 750/73.

U cilju utvrđivanja promene električne provodljivosti i elektrohemijskih parametara osnovnog materijala i zavarenog spoja u korozionim sredinama u zavisnosti od promene mikrostrukture usled zavarivanja, izvršena su metalografska ispitivanja zavarenog spoja na optičkom mikroskopu, merenje električne provodljivosti i elektrohemijskih parametara osnovnog materijala i zavarenog spoja.

The paper was published in its original form in the Proceedings of the 32nd Conference with international participation "Welding 2022" held in Tara, Serbia from October 12 to 15, 2022.

1. Introduction

The friction stir welding (FSW) process was developed and patented by the British Welding Institute- TWI, in December 1991 [1, 2].

The FSW procedure is process of joining materials in a solid state using the appropriate tool, without melting, protective armor and without the use of additional material. The resulting joint is a consequence of the effect of mechanical work and generated heat [3, 4]. During FSW welding due to simultaneous deformation and recrystallization processes (static and/or dynamic), and depending on the combination of applied parameters of the welding process, there is intense crushing of grains in the joint structure. Characteristic parts of the joint created by FSW are: TMAZ- thermo-mechanical affected zone, HAZ- heat affected zone and "nugget zone"- fine grain recrystallized area. The main welding parameters are tool travel speed (welding speed), $\mathbf{V_{tr}}$, and tool rotation rate, $\mathbf{V_{rot}}$ [3, 5].

Thermo-mechanical affected zone (TMAZ) is the part of the base metal that is simultaneously exposed to the effect of elevated temperature and the effect of mechanical load. In the structure, deformed, elongated grains which follow the flow of material mixing during the welding process can be clearly observed. Also, due to the influence of the heat effect, the grains may become coarse.

Heat affected zone (HAZ) is an area that is exposed to the effect of elevated temperature, but is not exposed to the effect of mechanical load. The heat effect can induce small scale phase transformation, such as grain coarsening and precipitation [6, 7, 8].

Nugget zone is a completely recrystallized area, which has a fine - grained structure, gained due to elevated temperature resulting from intense plastic deformation during welding [3, 5, 6]. Electrical conductivity is sensitive to structural changes. It depends on the amount of elements in the solid solution and the amount and nature of the sediment particles. Electrical conductivity also depends on grain size. Each grain boundary represents an obstacle for the movement of electrons, which means that by reducing the grain size, the electrical conductivity also decreases [8]. It is well known that 2024 aluminum alloy possesses moderate yield strength and good damage tolerance while 5083 aluminum alloy has good balance between light weight and corrosion resistance [9].

The aim of this work is to examine the influence of the change in the microstructure of the butt welded joint of two plates, made of different aluminum alloys (2024 - T351 and 5083 - H111), by the FSW process, on electrical conductivity and electrochemical parameters in corrosive environments.

2. Experimental part

Two plates, 65 mm wide, 500 mm long and 6 mm thick, made of dissimilar aluminum alloys are butt welded using a FSW method. The following parameters were used for welding: tool rotation rate, V_{rot}, was 750 rpm and tool travel speed (welding speed), V_{tr} , was 73 mm/min. The chemical composition of aluminum alloys 2024-T351 and 5083- H111 is shown in Table 1.

Table 1. *Chemical composition of AA2024 and AA5083 plates.*

Tabela 1. *Hemijski sastav ploča AA2024 i AA5083.*

Alloy	Element , (mass. %)								
	Mg	Mn	Si	Fe	Cu	Cr	Zn	Ti	Al
AA2024	1,45	0,60	0,06	0,16	4,28	0,003	0,08	0,03	rest
AA5083	4,60	0,55	0,24	0,24	0,07	0,10	0,07	0,02	rest

2.1 Macrostructure and microstructure analyses

Macrostructural and microstructural examinations of the welded joint were performed on samples taken from a cross-section in relation to the direction of the welded joint. The specimen for macrostructure was then mechanically ground using sand papers with grit sizes P240 to P2500. The macrostructure was revealed by etching in Tucker's reagent (45ml HCl, 15ml HNO_3, 15ml HF, 25ml H_2O) for 5 seconds.

The microstructure was observed on an optical microscope. The specimen for microstructure was mechanically ground using sand papers with grit sizes P240 to P4000, mechanically polished with the use of a diamond polishing suspensions with particle sizes of 7/5 μm, 5/3 μm и 3/2 μm. Subsequently, the specimens were electrochemically polished and etched. Electrochemical polishing of specimen was carried out using a perchloric acid-based solution (200 ml ethanol, 35 ml H_2O, 10 ml 60% solution of $HClO_4O$)

at 25 V for 8 seconds. The electrochemically etched using Barker's reagent (5 g HBF_4 (48%), 200 ml H_2O) at 12 V for 120 seconds.

2.2 Measurement of electrical conductivity

Electrical conductivity was measured on the "Förster SIGMATEST D 2.068" device in % IACS (International Anneald Copper Standard) units. All measurement was performed at room temperature at a test frequency of 120 Hz.

2.3 Corrosion test

The corrosion tests were conducted on the base materials, AA2024-T351 and AA5083-H111, as well as on the face and root of the welded joint. The areas exposed to the electrolyte were 1cm^2 for all measured zone. All the experiments were conducted in 3.5 % NaCl solution at room temperature (25 ± 2 ºC).

All experiments were carried out using a three-electrode system. A saturated calomel electrode (SCE), a large platinum sheet, and a measured zone with the area of 1 cm^2 were served as a reference electrode (RE), counter electrode (CE), and working electrode (WE), respectively.

3. Results

3.1 Macrostructure and microstructure

The characteristic macrostructure of the cross-section of the joint and the position of its areas (nugget, TMAZ, HAZ and base metals, BM) are shown in Figure 1. The thermo-mechanical affected zone (TMAZ) with pronounced deformed grains, a nugget with recognizable ring structure, and sleeve. The area of HAZ is poorly defined and cannot be clearly observed. Microstructures of base metals are shown in Figure 2.

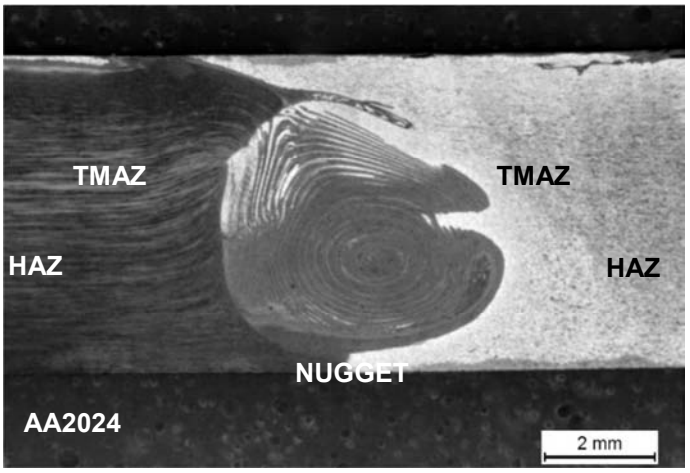

Figure 1. *The macrostructure of cross- section of welded joint.*

Slika 1. *Makrostruktura poprečnog preseka zavarenog spoja.*

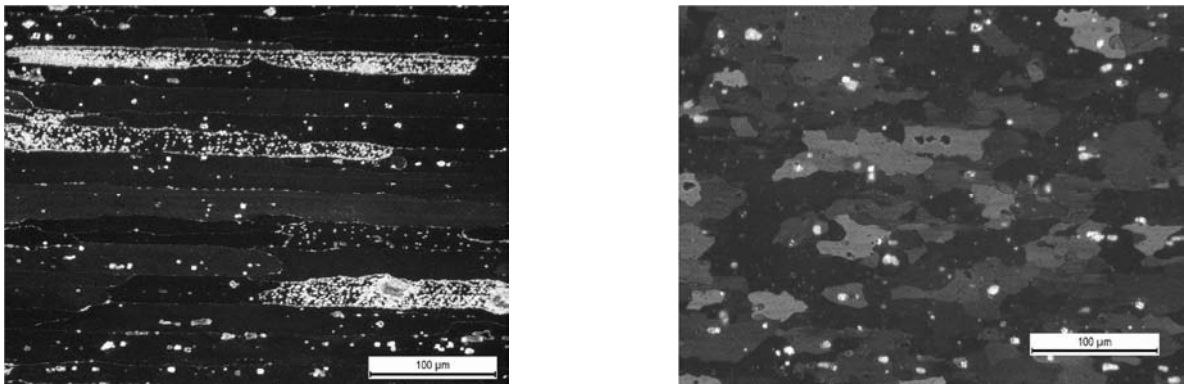

a) b)

Figure 2. *Microstructures of base metals: a) AA2024- T351 and b) AA5083- H111.*

Slika 2. *Mikrostrukture osnovnih metala: a) AA2024- T351 i b) AA5083- H111.*

The microstructure of aluminum alloy 2024-T351 is characterized by elongated grains, which is a consequence of the rolling process, while in alloy 5083- H111 the mechanical direction of the grains

is less pronounced. The microstructures of the welded joint zones are shown in Figures 3-5.

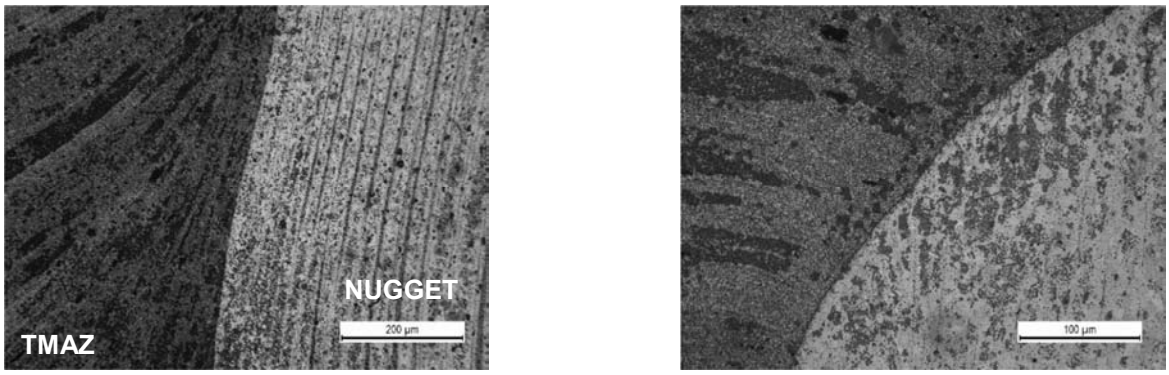

Figure 3. *The microstructure of the welded joint on the side of alloy 2024 at the border of TMAZ- nugget.*

Slika 3. *Mikrostruktura zavarenog spoja na strani legure 2024 na granici TMAZ-sočivast šav.*

The microstructure of the welded joint is inhomogeneous. Grains of different sizes and orientations can be observed in different parts of the welded joint. Figure 3 shows the microstructure of the welded joint on the side of alloy 2024. In TMAZ grains are strongly deformed and elongated in the direction of material flow during the welding process, while small and recrystallized grains are characteristic of the nugget zone.

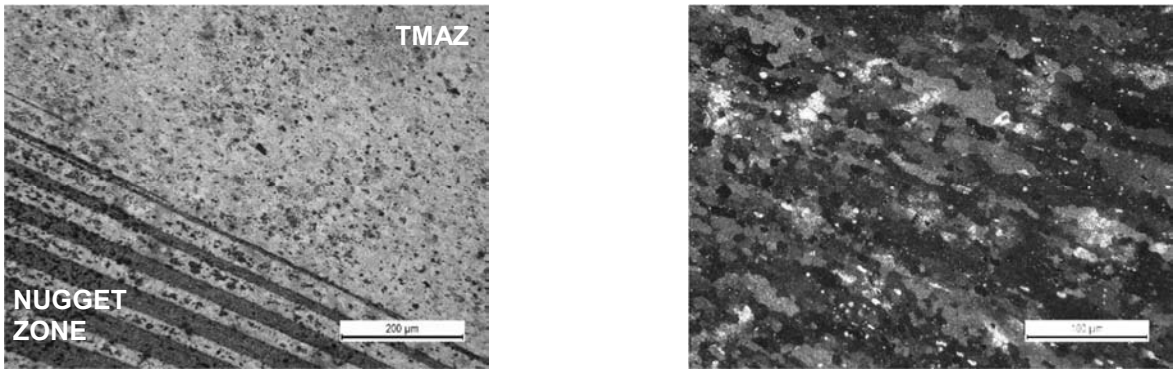

a) b)

Figure 4. *The microstructure of the welded joint on the side of alloy 5083: a) the border of TMAZ- nugget and b) TMAZ.*

Slika 4. *Mikrostruktura zavarenog spoja na strani legure 5083: a) granica TMAZ- sočivast šav i b) TMAZ.*

Figure 4 shows the microstructure of the weld joint on the side of alloy 5083. Deformed and elongated grains are clearly visible in the thermo-mechanical affected zone, Figure 4b.

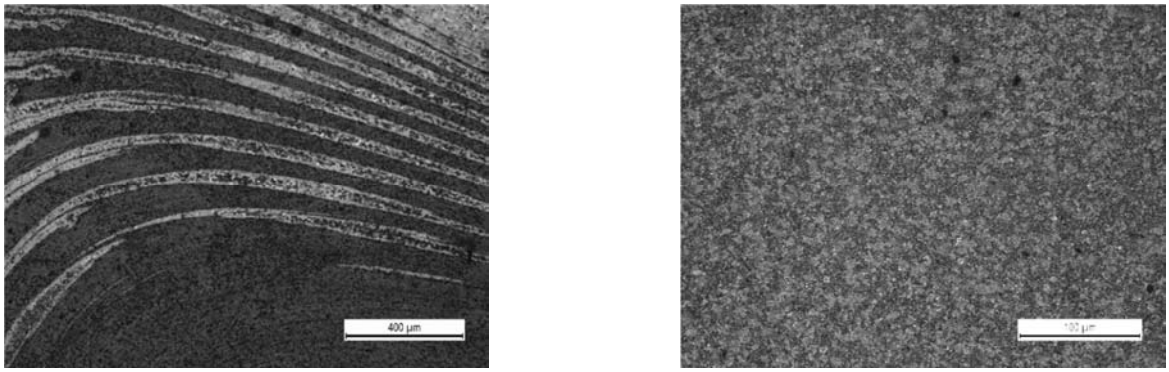

a) b)

Figure 5. *The microstructure of the welded joint- nugget zone at different magnifications.*

Slika 5. *Mikrostruktura zavarenog spoja –sočivastog šava pri različitim uvećanjima*

The appearance of a ring structure, which is shown in Figure 5 a) is characteristic of the nugget zone. In the nugget zone, the expected complete recrystallization of grains occurred.

3.2 Electrical conductivity

Electrical conductivity was measured on the FSW specimens in different zones of the surface of the joints, as shown in Figure 6. Zones 4-5 represent the weld metal, while zone 5 represent nugget zone. Figure 7 shows the change in electrical conductivity through the welded joint. On the x- axis, Figure 7, are marked the zones where electrical conductivity was measured, which are shown in Figure 6.

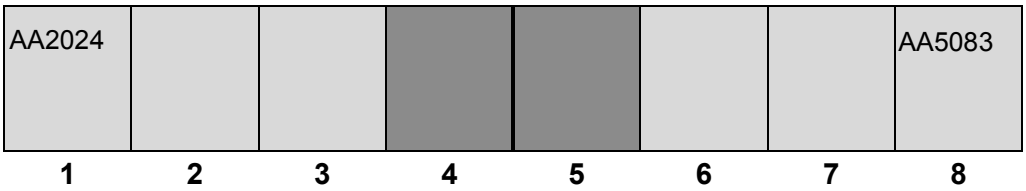

Figure 6. *Zones of the welded specimen for measuring electrical conductivity.*

Slika 6. *Zone zavarenog uzorka za merenje električne provodljivosti.*

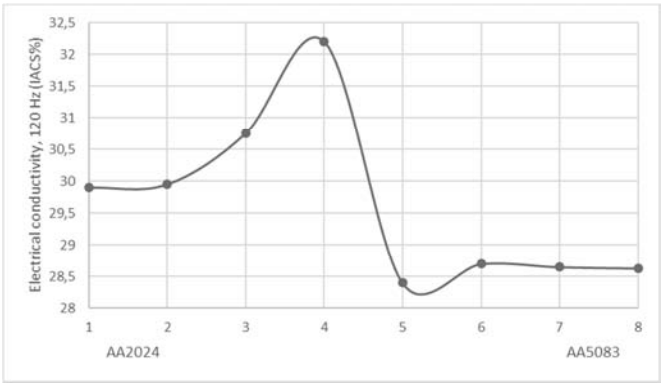

Figure 7. *The change in electrical conductivity of the welded joint.*

Slika 7. *Promena električne provodljivosti zavarenog spoja.*

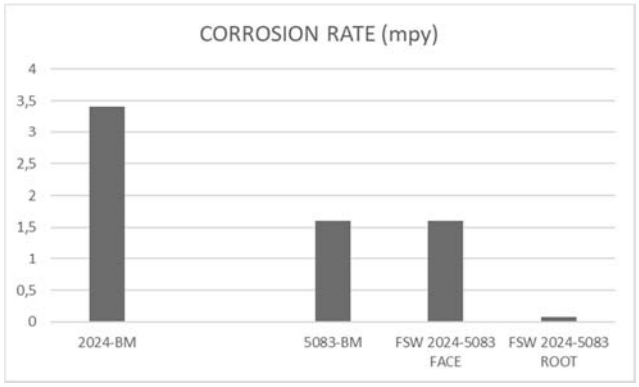

Figure 8. *Corrosion rate (CR) values of the measured zones.*

Slika 8. *Vrednosti brzine korozije (CR) merenih zona.*

The precipitation strengthened alloy 2024 - T351 has a higher electric conductivity than alloy 5083 - H111. The highest electrical conductivity was observed in TMAZ from the side of alloy 2024, while the lowest electrical conductivity was observed in nugget zone, where the grain is the smallest. Also, a slight increase in electrical conductivity is observed in TMAZ on the side of alloy 5083.

4. Conclusions

The values of thermal and electrical conductivity at room temperature mainly depend on the type of alloying elements and their concentration in solid solution and outside it, on the grain size and the concentration of other defect in the crystal lattice. With the decrease in grain size, a decrease in electrical conductivity is recorded, as a consequence of the increase in the number of boundaries that are obstacles to the movement of

3.3 Corrosion resistance

Corrosion rate values (CR) obtained from the potentiodynamic polarization curves for the measured zones are presented in Figure 8. Alloy 2024 has a higher corrosion rate than alloy 5083. The face of the weld metal has an approximate corrosion rate value as alloy 5083, while the root of the weld metal has the lowest corrosion rate value.

4. Zaključci

Vrednosti toplotne i električne provodljivosti na sobnoj temperaturi uglavnom zavise od vrste legirajućih elemenata i njihove koncentracije u čvrstom rastvoru i van njega, od veličine zrna i koncentracije drugog defekta u kristalnoj rešetki. Sa smanjenjem veličine zrna beleži se smanjenje električne provodljivosti, kao posledica povećanja broja granica koje su prepreka kretanju elektrona. Povećanje električne provodljivosti može biti

electrons. The increase in electrical conductivity may be due to the increase in grain size in HAZ and TMAZ, while the decrease in electrical conductivity is related to the fine - grained structure of the nugget.

The corrosion behavior of the friction-stir-welded joints of AA 2024-T351 and AA 5083-H111 was investigated and discussed by potentiodynamic measurements. The obtained results showed that AA 2024 has much lower corrosion resistance than AA 5083.

The highest corrosion resistance is in the root of the weld metal, which is a completely recrystallized area, with a fine- grained structure, gained due to elevated temperature resulting from intense plastic deformation during welding.

This phenomenon of the effect of temperature increase due to intense plastic deformation during welding on the corrosion resistance of welded joints should be the subject of further research.

posledica povećanja veličine zrna u HAZ i TMAZ, dok je smanjenje električne provodljivosti povezano sa sitnozrnom strukturom sočivastog šava.

Korozivno ponašanje spojeva zavarenih trenjem alatom AA 2024-T351 i AA 5083-N111 je ispitano i diskutovano potenciodinamičkim merenjima. Dobijeni rezultati su pokazali da AA 2024 ima mnogo manju otpornost na koroziju od AA 5083.

Najveća otpornost na koroziju je u korenu metala šava, koji je potpuno rekristalizovana površina, sa finozrnom strukturom, koja se dobija usled povišene temperature usled intenzivne plastične deformacije tokom zavarivanja.

Ovaj fenomen uticaja povećanja temperature usled intenzivne plastične deformacije pri zavarivanju na korozionu otpornost zavarenih spojeva treba da bude predmet daljih istraživanja.

References / Literatura

[1] S. K. Tiwari, D. K. Shukla, R. Chandra, (2013): Friction Stir Welding of Aluminum Alloys: A Review, International Journal of Mechanical, Aerospace, Industrial and Mechatronics Engineering Vol 7, No 12, 1315- 1320.

[2] R. Nandan, T. DebRoy, H.K.D.H. Bhadeshia, (2008): Recent advances in friction-stir welding – Process, weldment structure and properties, Progress in Materials Science, 53, 980–1023.

[3] I. Radisavljević, (2014): Uticaj parametara zavarivanja na svojstva zavarenih spojeva aluminijumskih legura dobijenih postupkom zavarivanja trenjem alatom, Ph. D. thesis, University of Belgrade, Belgrade, Serbia,

[4] D. Veljić, N. Radović, A. Sedmak, M. Petrović (2010): Tehnologija zavarivanja aluminijumskih legura postupkom zavarivanja trenjem alatom, Zavarivanje i zavarene konstrukcije, 55, 13-20.

[5] G. Cam , Selcuk Mistikoglu, Recent Developments in Friction Stir Welding of Al-alloys, Journal of Materials Engineering and Performance, April 2014.

[6] P. L. Threadgill, (2007): Terminology in friction stir welding, Science and Technology of Welding and Joining, VOL 12, NO 4, 357- 360.

[7] Threadgill, P.L., Leonard, A.J., Shercliff, H.R., Withers, P.J. (2009): Friction stir welding of aluminium alloys. Int. Mater. Rev. 54 (2), 49–93.

[8] T.G. Santos, P. Vilac, R.M. Miranda, (2011): Electrical conductivity field analysis for evaluation of FSW joints in AA6013 and AA7075 alloys, Journal of Materials Processing Technology, 211, 174-180.

[9] Peng-liang NIU, Wen-ya LI, Yu-hua CHEN, Qi-peng LIU, Dao-lun CHEN, (2022), Base material location dependence of corrosion response in friction-stir-welded dissimilar 2024-to-5083 aluminum alloy joints,Trans. Nonferrous Met. Soc.China, 32, .2164−2176.